International Journal of Adhesion & Adhesives 48 (2014) 295–302

Contents lists available at ScienceDirect

International Journal of Adhesion & Adhesives

journal homepage: www.elsevier.com/locate/ijadhadh

Beneficial in-situ incorporation of nanoclay to waterborne PVAc/PVOH dispersion adhesives for wood applications

Pablo J. Peruzzo [a], Audrey Bonnefond [a], Yuri Reyes [a], Mercedes Fernández [b], Joanna Fare [c], Erik Ronne [c], María Paulis [a,*], Jose R. Leiza [a,1]

[a] POLYMAT, Kimika Aplikatua Saila, Kimika Zientzien Fakultatea, University of the Basque Country UPV/EHU, Joxe Mari Korta Zentroa, Tolosa Hiribidea 72, 20018 Donostia-San Sebastián, Spain
[b] POLYMAT, Polimeroen Zientzia eta Teknologia Saila, Kimika Zientzien Fakultatea, University of the Basque Country UPV/EHU, Joxe Mari Korta Zentroa, Tolosa Hiribidea 72, 20018 Donostia-San Sebastián, Spain
[c] AkzoNobel, Sickla Industriväg 6, SE-131 34 Nacka, Sweden

ARTICLE INFO

Article history:
Accepted 9 September 2013
Available online 19 October 2013

Keywords:
Clay
(Mini)emulsion polymerization
Wood adhesives
Water and heat resistance

ABSTRACT

Nanoclay/polyvinyl acetate waterborne adhesives were prepared by using a two-step polymerization process. First, seed polymer particles containing the clay were obtained by batch miniemulsion polymerization. Then, the clay was buried within the particles by the addition of a neat monomer in the second step. The final stable dispersions could have up to 50 wt% of solids content. TEM images clearly showed the presence of clay inside the polymer colloids, although not totally exfoliated. The addition of nanoclay produced adhesives with higher water and heat resistance judged by the water swelling behavior and thermal degradation properties, which was reflected also in their better adhesive performance under wet conditions (D3 tests according to EN204) and high temperatures (WATT91) of the samples containing clay with respect to the pristine dispersions.

1. Introduction

Wood has an intrinsic potential to fulfill the criteria for being a competitive and sustainable engineering material, i.e. a renewable resource available in vast quantities and formed as a natural composite with an extraordinary high strength-to-weight ratio. However, for outdoor use it is necessary to enhance the performance and long-term durability of wood-based materials and the products related with their production, like coatings and adhesives.

The most commonly used adhesives in wood applications are the thermoset formaldehyde-based adhesives (urea–formaldehyde – UF, melamine–formaldehyde – MF, phenyl-formaldehyde, and resorcinol–formaldehyde) which have achieved low formaldehyde emissions [1]. Waterborne poly(vinyl acetate) (PVAc) dispersions stabilized with poly(vinyl alcohol) (PVA) have been used in wood adhesive for more than 50 years due to their good performance and competitive cost [2,3]. However, since water is a plasticizer for both polymers, these adhesives have low mechanical performance in warm and humid environments [4]. European Standard EN-204 gives the description and the minimal requirements that the PVAc adhesives must fulfill. D1 adhesives show a good resistance only under dry conditions; D2 adhesives should withstand a rather low water presence; D3 adhesives are suitable in the case of contact with cold water; and D4 adhesives are suitable to be used under extreme conditions (resistance to hot water) [5]. Conventional PVAc polymers can be used to formulate standard D1 or D2 adhesives. In general, the performance of these PVAc adhesives is improved to achieve a D3 or D4 performance either by using specific functional comonomers in the emulsion polymerization, by including polyvalent metal salts in the adhesive formulation, or by post-addition of thermosetting resins such as UF, MF or polyisocyanates for two-component systems, which rises the price of the final adhesive [6,7], makes the application process more complex for the end user, and may lead to formaldehyde emissions.

Functional engineered nanoparticles can also be introduced into water-based wood adhesives in order to improve the properties of wood–adhesive joints. The cost of the improved adhesives is a very critical parameter; thus the identification of cheap sources of nanoparticles will have priority. Nanoclays would be ideal systems due to their natural availability and low cost. Nanoclays have been used together with polymers in nanocomposites for a long time [8]. It has been found that these nanocomposite materials are superior to conventional unfilled materials with respect to the mechanical properties, thermal stability and barrier properties. In the case of water resistance, it has been proved that the organically modified clays have produced a reduction in the water uptake and water vapor permeation rates of polymer/clay nanocomposites [9–11]. On the other hand, it has been previously found that nanoclay can improve the mechanical properties of thermoplastic adhesives too

* Corresponding author. Tel.: +34 943 018481; fax: +34 943 017065.
E-mail addresses: maria.paulis@ehu.es (M. Paulis), jrleiza@ehu.es (J.R. Leiza).
[1] Tel.: +34 943 015329; fax: +34 943 017065.

0143-7496/$ - see front matter © 2013 Elsevier Ltd. All rights reserved.
http://dx.doi.org/10.1016/j.ijadhadh.2013.09.042

(for example improvement of the shear strength) [12–15]. For these improvements, it is important that the nanoparticles are compatible with the polymer matrix and are well dispersed. However, by conventional emulsion polymerization the exfoliation and dispersion of clay are limited, usually producing armored latex particles at low solids content [16–18].

Miniemulsion polymerization technology seems to be more appropriate to obtain encapsulated morphologies [19,20]. Upon mixing the aqueous and organic phases, and by applying energy to reduce the size of the droplets of the coarse emulsion, a stable dispersion of nanodroplets containing clay platelets is obtained. This miniemulsion can be polymerized to produce a latex where ideally the clay platelets would be encapsulated inside the polymer particles. Nevertheless, obtaining polymer particles with exfoliated clay incorporated into polymer particles (encapsulated or engulfed morphologies) is elusive. Although the hydrophilic nanoclay particles are usually modified with an organic molecule for its optimal dispersion in a lipophilic polymer matrix, difficulties arise from the fact that organically modified clays (OMC) cannot show full compatibility with the monomers, leading to phase separation [21]. Additionally, the aspect ratio of some clays (>150) makes their incorporation difficult in the typical range of particle sizes obtained in miniemulsion polymerization [21,22]. Furthermore, the stability of the latexes at high solids content cannot be guaranteed without using a very high amount of emulsifier concentration that in turn reduces the particle size of the miniemulsion droplet and decreases the properties of the latex films [23].

In a previous work a two-step polymerization approach to encapsulate clay within polymer colloids based on PVAc/PVA with 50 wt% of solids content was presented [24]. In this paper, the synthesis of new nanoclay–PVAc/PVA dispersions with a high solids content is presented in order to verify if the extensive encapsulation of clay is beneficial for the PVAc adhesive applications. A commercial organomodified clay was used, and the final clay content was varied between 0.3 and 1.7 wt% with respect to the solids of the dispersion (50 wt%). The morphology of the particles and films was studied by transmission electron microscopy and X-ray diffraction was used to study the degree of exfoliation of the clay platelets. Thermal, water sorption, mechanical and adhesive properties of films obtained from the dispersions were also studied to demonstrate that the presence of clay is beneficial for adhesive performance of these materials under hot and wet conditions.

2. Experimental

2.1. Reagents

Commercial organomodified clay, Dellite® 43B, was provided by Laviosa Chimica Mineraria S.p.A. and was used as received. It is a nanoclay derived from a naturally occurring montmorillonite specially purified and modified with a quaternary ammonium salt (dimethyl benzylhydrogenated tallow ammonium) [25]. The monomer, vinyl acetate (VAc), was used as received from Quimidroga. The poly (vinylalcohol)s, PVAs, Mowiol 23-88 and Mowiol 28-99 were kindly provided by Kuraray. A mixture comprising Mowiol 23-88 and Mowiol 28-99 at 3/1 weight ratio was used. Potassium persulfate, KPS, and sodium bicarbonate, both from Aldrich, were used as received.

2.2. Polymerization

Scheme 1 shows a picture of the process used during the synthesis. In the first step, batch miniemulsion polymerization is used to produce a seed polymer that contains all the clay; then, in step 2 the rest of the monomer is added to obtain a solids content of 50 wt%. The polymerization was carried out using the formulation shown in Table 1. The desired amount of clay was dispersed in the monomer (corresponding to "Step 1" in Table 1) by 5 min of ultrasonication (Branson Sonifier 450, operating at 8-output control and 80% duty cycle for 5 min) and magnetic stirring overnight. The PVA aqueous solution (obtained by dissolving the PVA at 90 °C for 2 h) and the buffer solution were mixed with the monomer/clay dispersion by magnetic stirring for 15 min. This mixture was used to prepare a miniemulsion by sonication (Branson Sonifier 450, operating at 8-output control and 80% duty cycle for 5 min) together with magnetic stirring. Then, the miniemulsion was loaded in a 0.5 L glass reactor, using mechanical stirring and nitrogen atmosphere. Once the system reached the desired temperature, 65 °C, the KPS initiator solution corresponding to the first step was fed for 5 min. This miniemulsion was left to react for 1 h (step 1). Once the seed polymer prepared by batch miniemulsion polymerization was obtained, the temperature was increased to 70 °C, and then the monomer and initiator solution corresponding to step 2 (see column "Step 2" in Table 1) were fed for 3 h. After the completion of feeding, a shot of initiator solution (2.25 g) was added and the latex was left at 70 °C for 1 h before cooling it down. A sample without clay was prepared for comparative purpose.

2.3. Characterization

Transmission electron microscopy, TEM (Tecnai G2 Twin), was used to analyze the structure of the particles. The films from the latexes were obtained in silicon molds at 23 °C and 55% of

Table 1
Formulation used in the synthesis of hybrid polymer particles.

Substance	Step 1 (g)	Step 2 (g)	Cooking (g)
Monomer (VAc)	56.45	136.05	–
Clay (Dellite® 43B)	Variable (0.00; 0.65; 2.00; 3.50)	–	–
Buffer ($NaHCO_3$) at 2.44 wt%	14.00	–	–
Initiator (KPS) at 1.6 wt%	28.55	13.80	2.25
PVA solution at 7.30 wt%	157.5	–	–

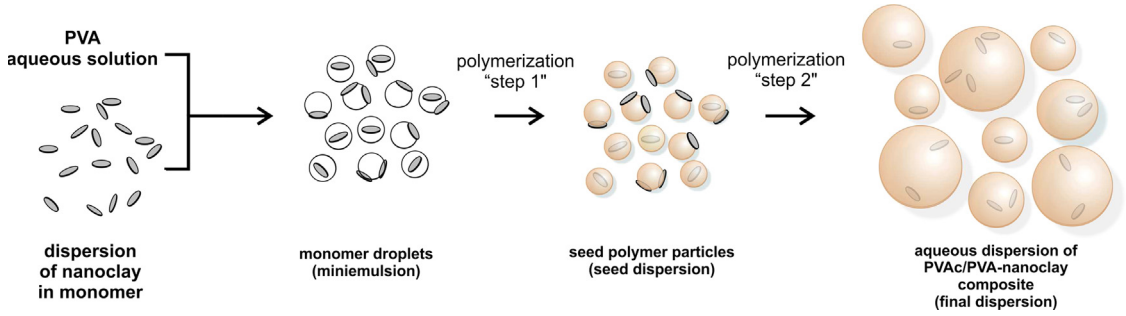

Scheme 1. Synthesis approach used in this work.

relative humidity. From these films, cross-sectional areas of about 100 nm of thickness were obtained by cryomicrotomy at −25 °C (Leica EM UC6). No staining agent was used in any of the samples. Wide-angle X-ray diffraction (WAXD) analyses were performed on a Philips PW 1729 Generator connected to a PW 1820 (Cu Kα radiation with wavelength $\lambda = 0.154056$ nm) at room temperature. Differential Scanning Calorimetry (DSC) was performed using a Shimadzu DSC-60 instrument, between −50 °C and +240 °C, at a heating rate of 10 °C min^{-1}. Samples were first heated to 100 °C at 30 °C min^{-1} and cooled down at 30 °C min^{-1} before scanning to erase thermal history. A nitrogen gas purge was applied and second heating curves were used for analysis. Thermogravimetric analysis, TGA, was obtained using a TA Instruments Thermogravimetric Analyzer model Q500, from 20 to 800 °C with a heating rate of 10 °C min^{-1} under nitrogen atmosphere; to degrade the organic components air was injected at 700 °C for 5 min.

For the water uptake measurements, two specimens of 20 mm diameter and 1 mm thickness for each condition were prepared and dried at 23 °C and 55% of relative humidity. They were immersed in distilled water at room temperature. Specimens were periodically removed from water, dried with filter paper and immediately weighed with a precision of 0.01 mg before returning them to the water bath. The relative mass uptake, M_t, was calculated using the following equation:

$$M_t(t) = \left(\frac{W_t - W_0}{W_0}\right) 100 \quad (1)$$

where W_t and W_0 are, respectively, the instantaneous and initial weights.

The dynamic viscoelastic behavior of samples was investigated using a stress controlled rotational rheometer ARG2 (TA Instruments) with parallel-plate geometry (12 mm diameter). Specimens of 12 mm diameter and 1 mm thickness were prepared and dried at 23 °C and 55% of relative humidity. Temperature sweep experiments in the linear regime were conducted under nitrogen atmosphere at 1 Hz; the cooling rate was 2 °C min^{-1} and temperature was varied from 150 to 60 °C. Prior to the measurement, the linear viscoelastic conditions were established by a torque sweep test and all tests were done under 0.1% deformation and 4 N normal force. Tensile shear strength of the samples was tested according to EN-204. Individual test specimens of $150 \times 20 \times 10$ mm^3 using beech wood (12 ± 1% moisture content) were prepared. The samples were glued

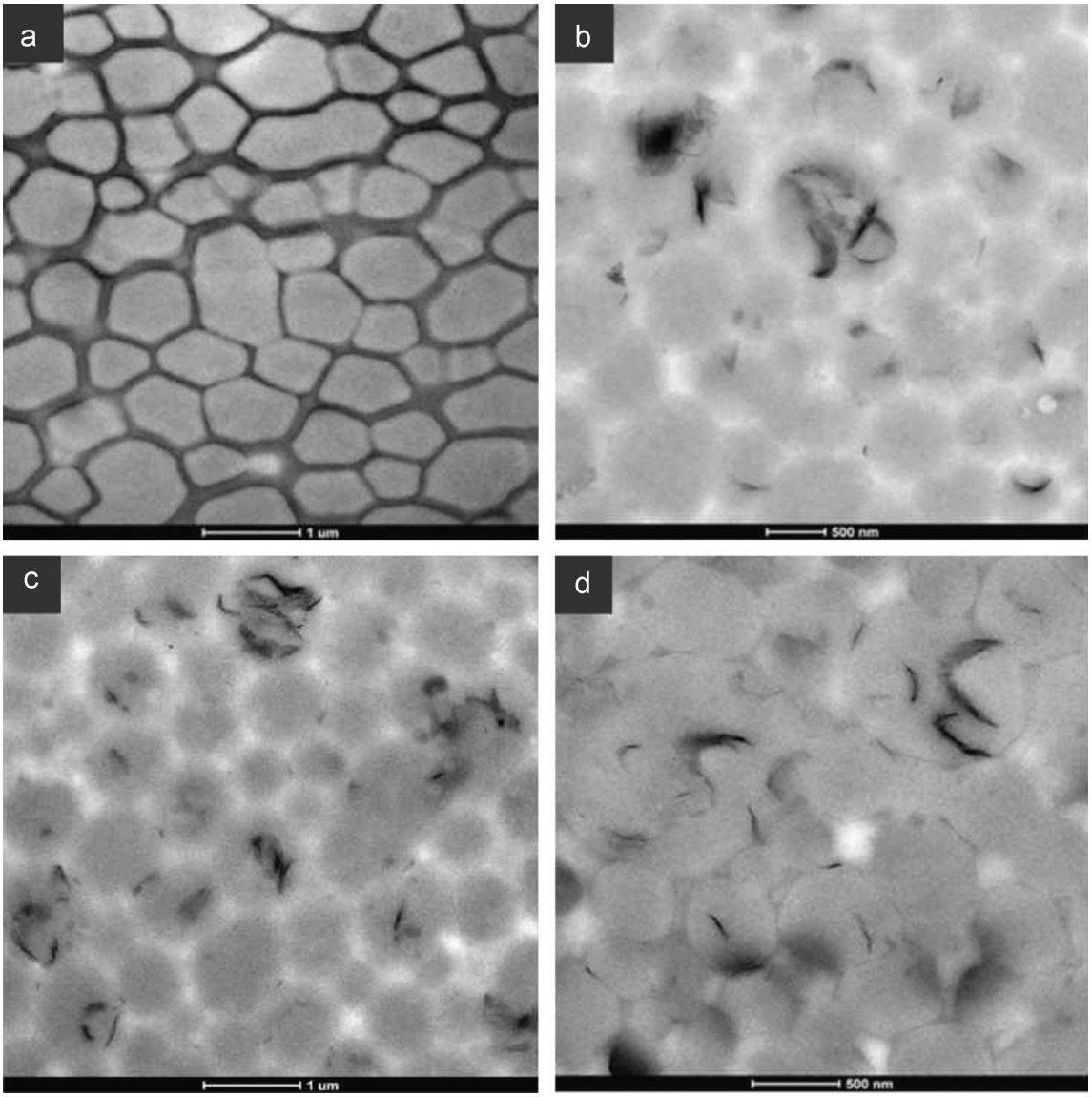

Fig. 1. TEM image of thin cross-sectional portions of the films obtained from the final latex of the blank sample (a) and samples containing 0.3 (b), 1.0 (c) and 1.7 wt% (d) of clay.

without any addition of coalescing agent or hardener. Pressing was performed at 50 °C for 1 h. The resulting lap joint test pieces were randomly distributed into four treatment groups: (1) 5 specimens were conditioned at 20 ± 2 °C and 65 ± 5% relative humidity for 7 days (durability class D1); (2) 8 specimens were conditioned under the above standard ambient conditions followed by storage of test specimen in cold water (at 20 °C) for 3 h and reconditioning for 7 days under standard ambient conditions (durability class D2); (3) 8 specimens were conditioned in the above standard atmosphere followed by 4 days in water at 20 ± 5 °C (durability class D3); and (4) 8 specimens were conditioned in the described standard atmosphere and then each test piece was heated for 1 h in a preheated fan oven at 80 °C (WATT91) [5,26,27]. The tensile shear strength was measured with an Alwetron TCT50 equipped with a load cell of 50 kN, at 20 ± 5 °C and 65 ± 5% relative humidity, and at 50 mm/min of loading rate.

3. Results and discussion

3.1. Morphology of the nanocomposites

The localization of clay in the synthesized polymer colloids was studied by TEM. Fig. 1 shows TEM images of thin cross-sections of films obtained from the dispersions prepared in this work. The polymer particles in the film retain their identity due to limited particle deformation and chain interdiffusion between neighboring particles, since the film was formed at a lower temperature (23 °C) than the glass transition temperature of the polymers (≈ 36–42 °C) [28]. It can be observed that particles are larger in size than the nanoclay; particles have a broad size distribution which is common in the systems that use PVA as protective colloid. It can also be observed that in many polymer particles there are aggregates of clay clearly within the polymer particles and only in few cases on the particle surface. Approximately 35% of the polymer particles contain clay.

Fig. 2 shows the WAXD results of the clays and nanocomposites prepared in this work. The OMC 43B (Fig. 2(a), bottom) has a diffraction peak at $2\theta = 4.9°$. It is determined that the intergallery space is 1.80 nm for the clay. No diffraction peaks were observed in the films without clay (blank sample, seed and final latex). However, a signal was observed for the films obtained from the hybrid seed latexes. A small diffraction peak was observed for the films obtained from the seed latexes of samples containing 0.3 and 1.0 wt% of clay content, while a clear signal appeared for the highest clay content. The higher the clay content the more prominent the peak, but at the three clay loadings the position of the peak was the same, which was located at $2\theta = 2.6°$, corresponding to an intergallery space of 3.53 nm, very similar to the one found by Corcione et al. for their intercalated Dellite 43B/polyurethane hybrids [25]. Therefore, during the seed synthesis, some growing polymer chains entered into the clay interlayer domains, increasing the interlayer space. Therefore at the end of the seed production, a clay intercalated structure was obtained in the polymer matrix. No peak was observed for the films of the final latexes. Although it could be attributed to the complete exfoliation of clay in the final material, there were some stacks of clay detected in the TEM images of the final films (Fig. 1). Therefore, the lack of diffraction peaks could be related to the low clay content in the final films (between 0.3 and 1.7 wt% with respect to the total solids), rather than to its complete exfoliation [29,30]. Note that in the seed latex with 0.9 wt% clay, the peak at 2.6° can be detected.

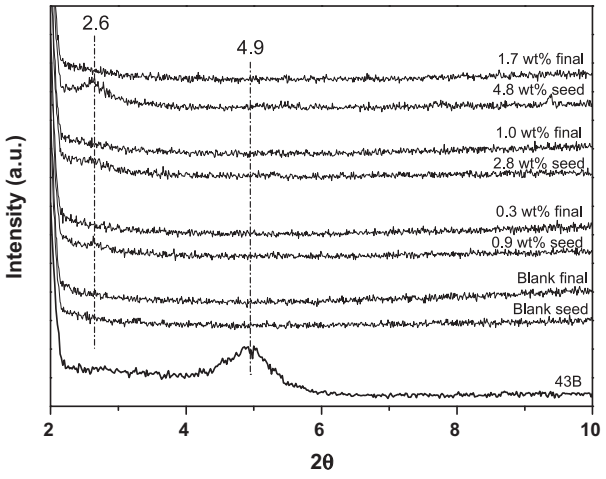

Fig. 2. WAXD results of clays and films obtained from the seed and final latex prepared in this work. The lines have been shifted to the *y*-axis for clarity.

3.2. Thermal behavior

DSC curves of the blank and samples with different clay contents are presented in Fig. 3(a). The DSC measurements revealed only one T_g at around 36 °C for the blank sample, at an intermediate T_g value between the T_g of the PVAc (≈ 28 °C) and the PVA polymers (≈ 80 °C) [31,32]. This means that there was an extensive grafting of the PVAc with the PVA during polymerization reaction. One T_g was also found for the hybrid composites. The T_g values of the nanocomposites were found to depend on the nanoclay content (see Table 2). The presence of clay at a composition of 0.3 wt% initially increased T_g of the polymer by around 7 °C (see Table 2). Usually, this increment of T_g is associated to a positive interaction of the polymer matrix with the filler, due to a shift of the dynamics of the chains close to the filler surface [33]. As clay content increased, the nanocomposites showed a decrease in T_g values. Here, the nonreactive modifier of clay could be acting as a plasticizer, resulting in a decrease in T_g with increasing clay content [34].

The TGA measurements of pure PVAc and nanocomposites containing clay are shown in Fig. 3(b). According to these findings, the thermal degradation of PVAc film and nanocomposites shows more than one degradation process [35]. The thermal decomposition behavior of the samples containing clay also passed through these three stages. A slight improvement in the thermal stability of the nanocomposites containing clay was found, as compared to the pure copolymer. The maximum decomposition temperature for the first step, $T_{d,max}$, calculated from the maximum of the derivative weight loss versus temperature curve, is also presented in Table 2. An increase of around 14 °C in the decomposition temperature was obtained for these hybrid samples compared to the counterpart without clay. Indeed, in the second and third steps a larger delay in the decomposition process can be observed for the samples containing clay. It may be attributed to the thermal isolation effect of the clay layers and the mass transport barrier provided to the volatile products generated during thermal decomposition [36]. From TGA measurement, the organic content of 43B clay is 38 wt% (result not shown). It can be noticed that the amount of the recovered clay (char column in Table 2) is in agreement with the theoretical filler amount for the nanocomposites (62% of 43B clay loaded amount). The slight discrepancies can be attributed to the heterogeneous distribution of clay during film formation.

3.3. Rheological properties

Fig. 4 shows the storage modulus G' and tan(δ) as a function of temperature. Above 60 °C (T higher than T_g of the polymer) the

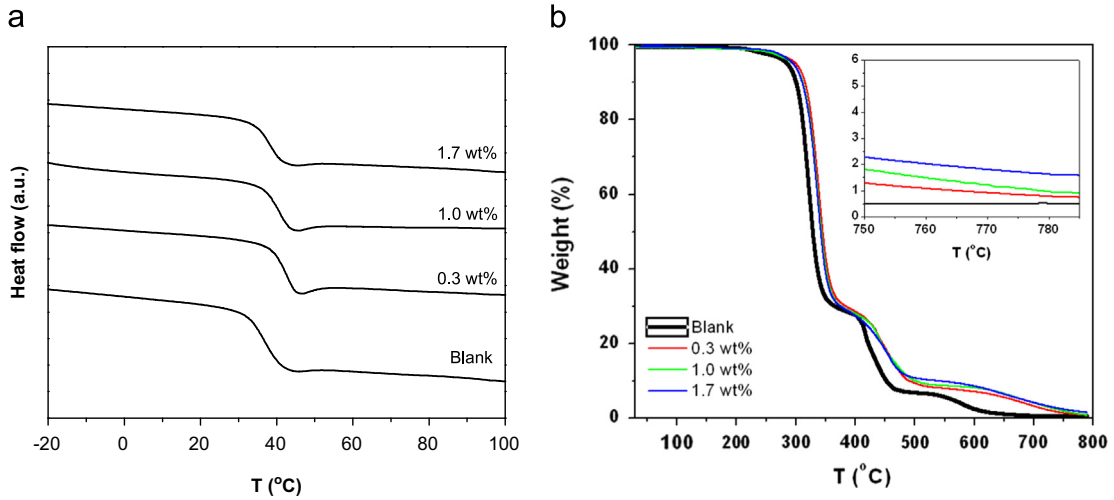

Fig. 3. DSC curves of the samples prepared in this work (a), and TGA thermograms of the blank and the nanocomposites with 0.3, 1.0 and 1.7 wt% of clay content (b).

Table 2
DSC and TGA results of the samples prepared in this work.

Clay content (wt%)	DSC	TGA			
	T_g (°C)	$T_{d,max}$ (°C)	Residue (wt%)	Char (wt%)[a]	Theoretical char[b] (wt%)
Blank	36	324	0.5	0.0	0.0
0.3	43	338	0.8	0.3	0.2
1.0	41	338	1.0	0.5	0.6
1.7	38	337	1.6	1.2	1.0

[a] Calculated using as reference the residue value of the blank sample.
[b] Calculated from the 43B load, taking into account the organic content of the OMC.

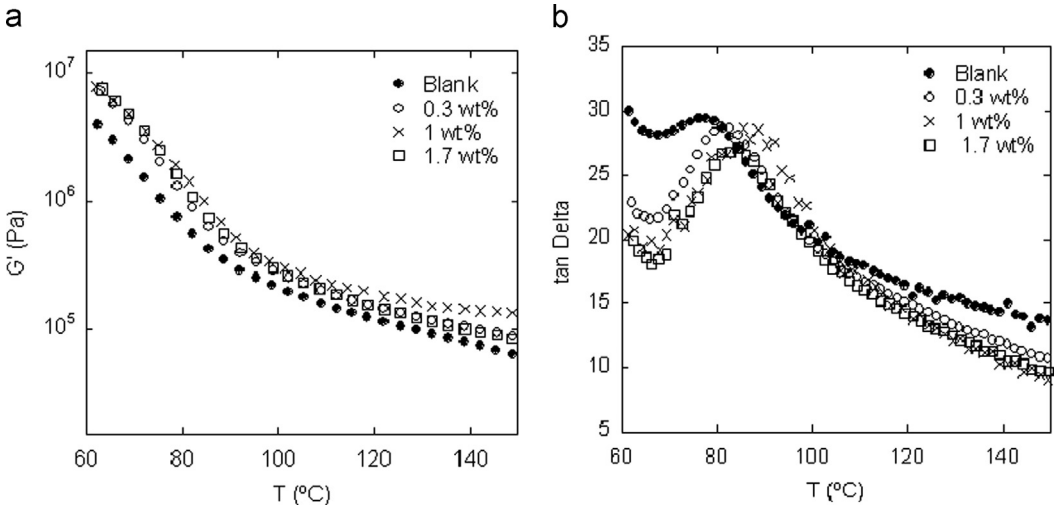

Fig. 4. Clay content effect on (a) storage modulus curves and (b) tan(δ).

storage modulus in the rubbery plateau ($T > 90$ °C) was enhanced with the incorporation of clay. This behavior could be attributed to the restriction on the polymer chain mobility due to the polymer–clay interactions. The G' modulus value at rubbery plateau initially increases until reaching the highest value at 1.0 wt% of filler content, and then decreases when the clay content increases at 1.7 wt%. The tan(δ) curves showed the presence of a peak around 80 °C for the unfilled polymer, which can be attributed to the glass transition of the PVA [37]. This transition was not observed by DSC probably due to the higher heating rate and to the low free PVA to grafted PVAc–PVA ratio in the samples. The curves of the nanocomposite samples revealed that this transition was initially shifted to higher temperature values with the incorporation of clay to the polymeric matrix up to 1.0 wt%, and then decreased with the incorporation of additional clay, similar to the trend observed before for the storage modulus value. These observations (the increase of the storage modulus value at the rubbery plateau and the shift of the PVA glass transition to higher temperatures) confirmed the presence of a positive interaction of the polymeric chains with the incorporated filler. It may be ascribed to the confinement of the polymer chains, which resulted from the strong interaction between the OMC and the polymeric matrix

as the clay content is below 1.0 wt%. However, for higher filler content, probably the partial agglomeration of clay, that reduced the polymer/clay interfacial area, resulted in the decrease in G' value.

3.4. Water uptake

The water sorption curves for the blank and the nanocomposite films are shown in Fig. 5(a). All the samples presented water sorption curves with an initial linear behavior before reaching a maximum, followed by a smooth leveling of the sorption curve to a saturation level at higher immersion time. The decrease in the relative mass uptake was probably due to the dissolution of salts and non-grafted PVA from the polymer film to the water bath. Qualitatively, a first remark is that the sample without clay was difficult to handle after 6 h of immersion in water. Additionally, this sample became soft and broke at 12 h of immersion (see the arrow in Fig. 5(a)), while all the samples containing clay were harder and could be manipulated without problems during the experiment (see pictures in Fig. 5(b)). The initial slope of the sorption curve of the blank specimen was higher than that of the specimens that contain clay, while the latest showed a similar initial water sorption rate regardless of the clay content. The decrease in the kinetics of water sorption of the nanocomposites related to the unfilled matrix was probably due to a barrier effect associated with the large platy-nanoclay particles that physically blocked the penetration of water molecules. The mass uptake at the maximum and at the saturation level is plotted in Fig. 5(c). The samples containing clay showed the maximum peak at higher immersion time than that of the pristine polymer. The general trend was a decrease in both values with increasing clay content; these parameters decreased as the clay content increased up to 1.0 wt%, with a minimum at this composition. The water sorption at the maximum increased with the incorporation of additional clay probably due to the formation of clay aggregates, indicating that an attempt to incorporate more clay than 1.0 wt% did not seem to be beneficial for the water resistance behavior either.

3.5. Adhesive properties

In order to evaluate the effect of the filler on the strength of wood joints, shear strength of joints bonded with different samples was measured in different essays. The results obtained from the evaluation of the adhesives properties EN 204-D1, D2, D3 and WATT91 of the samples prepared in this work are presented in Fig. 6 and Table 3.

3.5.1. Dry state and re-dried state (D1 and D2)

The results of the D1 test (adhesives for interior use, moisture content of wood does not exceed 15%) are presented in the upper-left hand side of Fig. 6. The results demonstrate that the samples had a very good bonding, where the average wood failure was 95–100% for all the samples (see Table 3). These percentages illustrate that the bonding quality is very good for these samples.

On the upper right-hand side the results of the D2 test (3 h of immersion in cold water and re-drying/ adhesives for interior use, occasional short-term exposure to water or moisture, moisture content of wood does not exceed 18%) are presented. The TSS did not show a clear dependency on the clay content, and none of the samples had a TSS $\geq$ 8 MPa, which is the lowest limit for a D2 adhesive. On the other hand the samples with 0.3 and 1.0 wt% of clay content showed a higher wood failure (79% and 69%, respectively) compared to samples bonded with pure PVAc adhesive (28%), indicating that the incorporation of clay prevents the damage of the joint during water exposure. An additional increase in the clay content produced a decrease in both the tensile shear strength and wood failure percentage, suggesting that a higher clay content is not beneficial for the adhesive properties after cold water exposure.

3.5.2. Wet state (D3) and elevated temperature (WATT91)

In the D3 test (4 days of immersion in cold water/ adhesives for interior use with frequent short-term exposure to water or high humidity) it was not possible to analyze the blank sample (with no

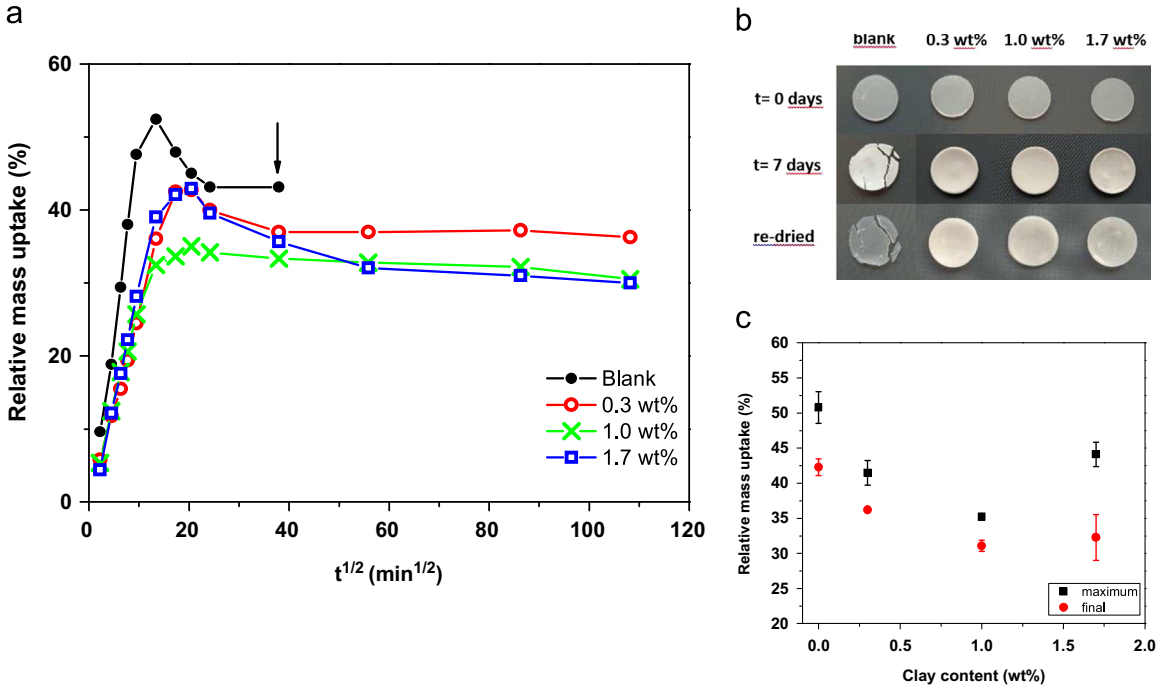

Fig. 5. (a) Relative water uptake, (b) pictures of water sorption specimens at $t=0$ days, $t=7$ days and re-dried specimens after water immersion for the blank and the nanocomposite samples, and (c) maximum and saturation water uptake values of the films obtained from the final latex prepared in this work. The arrow shows the time at which the specimen of blank sample was broken during the experiment.

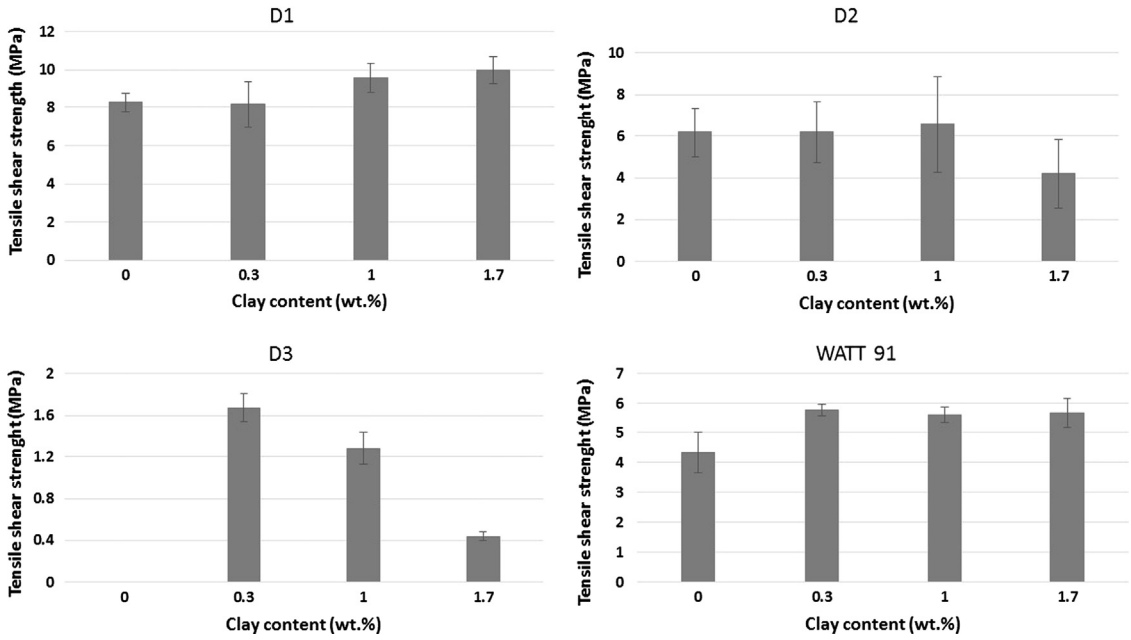

Fig. 6. Tensile shear strength results for the samples prepared in this work according to EN 204-D1, D2, D3 and WATT91.

Table 3
Percentage of wood failure for the samples under different conditions.

Sample	D1	D2	D3	WATT91
Blank	100	28	0	0
0.3 wt%	100	79	0	10
1.0 wt%	100	69	0	0
1.7 wt%	97	0	0	0

clay) due to delamination of all the samples during water exposure. Concerning the TSS values, the highest value was observed for the sample with 0.3 wt% of clay content, and then they decreased as the clay content increased. Although samples did not pass the D3 class standard (>2 MPa), this result showed that incorporation of filler had a positive effect on the water resistance of these adhesives.

Finally, for the WATT91 test (heating the test specimen for 1 h at 80 °C), the TSS of the polymers with clay was larger than that for the blank system; however, there was no effect of the amount of clay, since the TSS values for the three clay loadings were equal within the experimental error. This means that all the samples showed an improvement in heat resistance of wood joints when compared with the blank sample. These results indicate that the addition of the organomodified clay to a PVAc/PVA latex by obtaining encapsulated nanocomposite materials effectively enhanced the water resistance and heat resistance of the glue line. The incorporation of clay produced some kind of reinforcing effect on the matrix. Such an effect could be related to a lower mobility of polymer, improving the adhesive properties that is in agreement with results previously shown in this work.

Collectively, the results presented in this work demonstrate that the encapsulation of the filler produces an adhesive material with enhanced properties, due to the positive interaction between the polymer chains and the OMC, in agreement with the DSC and rheological measurements. The clay platelets present within the polymer particles act as a heat and water barrier, reducing the water sorption kinetics and improving the thermal stability of these nanocomposites, resulting in an enhancement of the adhesive properties under warm and wet conditions. It is noticed that the samples that exhibit the best global performance are the samples with lower clay content. Indeed, probably due to partial aggregation phenomena of the inorganic filler, the incorporation of additional clay produced a negative effect on the nanocomposite properties and, consequently, on the adhesive properties. Therefore, this work demonstrates that efforts directed to increase the exfoliation of clay within the polymer particles might produce, if achieved, PVAc adhesives with even higher adhesive performance at higher clay contents.

4. Conclusions

By using a two-step polymerization process it was possible to obtain clay encapsulated within polymer colloids dispersed in water at high solids content. TEM images clearly show the presence of clay inside the polymer colloids, although not totally exfoliated. The approach described in this paper led to the production of polymeric materials with enhanced properties, such as higher water resistance and improved thermal and adhesives properties, if compared with the pristine polymer. The results clearly demonstrate that the presence of clay encapsulated within polymer particles is beneficial in order to obtain better properties of waterborne PVAc adhesives for more demanding applications.

Acknowledgment

The authors acknowledge the funding by the University of the Basque Country UPV/EHU (UFI11/56), Basque Government (GV IT373-10), Ministerio de Ciencia e Innovación (MICINN, Ref. CTQ2011-25572) and European Union (Woodlife project FP7-NMP-2009-SMALL-246434). The sGIKer UPV/EHU is also gratefully acknowledged for the electron microscopy facilities of the Gipuzkoa unit. PJP is a member of CONICET.

References

[1] Frihart CR. Wood adhesion and adhesives. In: Rowell Roger M, editor. Handbook of wood chemistry and wood composites. Boca Raton: CRC Press; 2005 [chapter 9].

[2] Tout R. A review of adhesives for furniture. Int J Adhes Adhes 2000;20:269–72.
[3] Stoeckel F, Konnerth J, Gindl-Altmutter W. Mechanical properties of adhesives for bonding wood – a review. Int J Adhes Adhes 2013;45:32–41.
[4] Qiao L, Easteal AJ. Aspects of the performance of PVAc adhesives in wood joints. Pigm Resin Technol 2001;30:79–87.
[5] EN 204. Classification of thermoplastic wood adhesives for non-structural applications. Brussels, Belgium: CEN, European Committee for Standardization; April 2002.
[6] Qiao L, Coveny PK, Easteal AJ. Modifications of poly(vinyl alcohol) for use in poly (vinyl acetate) emulsion wood adhesives. Pigm Resin Technol 2002;31:88–95.
[7] Kaboorani A, Riedl B. Improving performance of polyvinylacetate (PVA) as a binder for wood by combination with melamine based adhesives. Int J Adhes Adhes 2011;31:605–11.
[8] Kojima Y, Usuki A, Kawasumi M, Okada A, Kurauchi T, Kamigaito O. Synthesis of nylon 6–clay hybrid by montmorillonite intercalated with ε-caprolactam. J Polym Sci A Polym Chem 1993;31:983–6.
[9] Diaconu G, Asua JM, Paulis M, Leiza JR. High-solids content waterborne polymer–clay nanocomposites. Macromol Symp 2007;259:305–17.
[10] Chen B, Liu S, Evans JRG. Polymeric thermal actuation using laminates based on polymer–clay nanocomposites. J Appl Polym Sci 2008;109:1480–3.
[11] Zulfiqar S, Ahmad Z, Sarwar MI. Preparation and properties of aramid/layered silicate nanocomposites by emulsion polymerization. Polym Adv Technol 2008;19:1720–8.
[12] Shaikh S, Birdi A, Qutubuddin S, Lakatosh E, Baskaran H. Controlled release in transdermal pressure sensitive adhesives using organosilicate nanocomposites. Ann Biomed Eng 2007;35:2130–7.
[13] Ray SS, Okamoto M. Polymer/layered silicate nanocomposites: a review from preparation to processing. Prog Polym Sci 2003;28:1539–641.
[14] Biswas M, Ray S. New polymerization techniques and synthetic methodologies, 155. New York: Springer; 167–222.
[15] Pavlidou S, Papaspyrides C. A review on polymer-layered silicate nanocomposites. Prog Polym Sci 2008;33:1119–98.
[16] Voorn D, Ming N, van Herk A. Clay platelets encapsulated inside latex particles. Macromolecules 2006;39:4654–6.
[17] Diaconu G, Paulis M, Leiza JR. Towards the synthesis of high solids content waterborne poly(methyl methacrylate-co-butyl acrylate)/montmorillonite nanocomposites. Polymer 2008;49:2444–54.
[18] Negrete-Herrera N, Putaux J-L, David L, Bourgeat-Lami E. Polymer/laponite composite colloids through emulsion polymerization: influence of the clay modification level on particle morphology. Macromolecules 2006;39:9177–84.
[19] Bonnefond A, Micusik M, Paulis M, Leiza JR, Teixeira RFA, Bon SAF. Morphology and properties of waterborne adhesives made from hybrid polyacrylic/montmorillonite clay colloidal dispersions showing improved tack and shear resistance. Colloid Polym Sci 2013;291:167–80.
[20] Aguirre M, Paulis M, Leiza JR. UV screening clear coats based on encapsulated CeO_2 hybrid latexes. J Mater Chem A 2013;1:3155–62.
[21] Reyes Y, Paulis M, Leiza JR. Modeling the equilibrium morphology of nanodroplets in the presence of nanofillers. J Colloid Interface Sci 2010;352:359–65.
[22] Micusik M, Bonnefond A, Reyes Y, Bogner A, Chazeau L, Plumer C, et al. Morphology of polymer/clay latex particles synthesized by miniemulsion polymerization: modeling and experimental results. Macromol React Eng 2010;43:432–44.
[23] Aramendia E, Mallegol J, Jeynes. C, Barandiaran MJ, Keddie JL, Asua JM. Distribution of surfactants near acrylic latex film surfaces: a comparison of conventional and reactive surfactants (surfmers). Langmuir 2003;19:3212–21.
[24] Reyes Y, Peruzzo PJ, Fernández M, Paulis M, Leiza JR. Encapsulation of clay within polymer particles in a high solids aqueous dispersion. Langmuir 2013;28(31):9849–56.
[25] Corcione CE, Prinari P, Cannoletta D, Mensitieri G, Maffezzoli A. Synthesis and characterization of clay-nanocomposite solvent based polyurethane adhesives. Int J Adhes Adhes 2008;28:91–100.
[26] EN-205 Adhesives. Wood adhesives for non-structural applications – determination of tensile shear strength of lap joints. Brussels, Belgium: CEN, European Committee for Standardization; 2003.
[27] EN-14257 Wood adhesives. Determination of tensile strength of lap joints at elevated temperature (WATT91). Brussels, Belgium: CEN, European Committee for Standardization; 2006.
[28] Keddie JL, Routh AF. Fundamentals of latex film formation: processes and properties. Dordrecht: Springer; 2010.
[29] Morgan AB, Gilman JW. Characterization of polymer-layered silicate (clay) nanocomposites by transmission electron microscopy and X-ray diffraction: a comparative study. J Appl Polym Sci 2003;87:1329–38.
[30] Drummy LF, Wang YC, Schoenmakers R, May K, Jackson M, Koerner OH, et al. Morphology of layered silicate–(nanoclay)–polymer nanocomposites by electron tomography and small-angle X-ray scattering. Macromolecules 2008;41:2135–43.
[31] Bandrup J, Immergut EH, Grulke EA. Polymer handbook. New York: Wiley-Interscience; 2003.
[32] Finch CA. Polyvinyl alcohol developments. West Sussex: John Wiley & Sons; 1992.
[33] Faucheu J, Gauthier C, Chazeau L, Cavaillé J-Y, Mellon V, Pardal F, et al. Properties of polymer/clay interphase in nanoparticles synthesized through in-situ polymerization processes. Polymer 2010;51:4462–71.
[34] Zengeni E, Hartmann P, Pasch H. Encapsulation of clay by ad-miniemulsion polymerization: the influence of clay size and modifier reactivity on latex morphology and physical properties. Appl Mater Interfaces 2012;4:6957–68.
[35] Holland BJ, Hay JN. The thermal degradation of poly(vinyl acetate) measured by thermal analysis – Fourier transform infrared spectroscopy. Polymer 2002;43:2207–11.
[36] Sapalidis AA, Katsaros FK, Kanellopoulos. NK. PVA/montmorillonite nanocomposites: development and properties, nanocomposites and polymers with analytical methods. In: Cuppoletti J, editor. Nanocomposites and polymers with analytical methods. Croatia: InTech; 2011. p. 29–50.
[37] López-Suevos F, Eyholzer C, Bordeanu N, Richter K. DMA analysis and wood bonding of PVAc latex reinforced with cellulose nanofibrils. Cellulose 2010;17:387–98.